



CHORUS

This is the accepted manuscript made available via CHORUS. The article has been published as:

Angular photonic band gap

Rafif E. Hamam, Ivan Celanovic, and Marin Soljačić
Phys. Rev. A **83**, 035806 — Published 21 March 2011
DOI: [10.1103/PhysRevA.83.035806](https://doi.org/10.1103/PhysRevA.83.035806)

Angular Photonic Band Gap

Rafif E. Hamam, Ivan Celanovic, and Marin Soljačić

*Center for Materials Science and Engineering and Research Laboratory of Electronics,
Massachusetts Institute of Technology, Cambridge, Massachusetts 02139, USA*

We present detailed numerical simulations of a novel class of material-systems that strongly discriminate light based primarily on the angle of incidence, over a broad range of frequencies, and independent of the polarization. Unique properties of these systems emerge from exploring photonic crystals whose constituents have anisotropic dielectric response.

Materials and structures that strongly discriminate electromagnetic radiation based on one, or more of its properties (e.g. polarization, frequency) play an enabling role for a wide range of physical phenomena. For example, polarizers can selectively transmit light based on its polarization¹ over a wide range of frequencies; photonic crystals² (PhCs) can reflect light of certain frequencies irrespective of the angle of incidence, and irrespective of the polarization. A material-system that could transmit light based primarily on the angle of incidence might also enable a variety of novel physical phenomena. Light incident at a prescribed range of angles would be nearly perfectly transmitted, while light from other angles of incidence would be nearly perfectly reflected (Fig. 1a). Ideally, such an angular selectivity would apply independent of the incoming polarization, and over a broad range of frequencies. Structures with such strong angular selectivity do not currently exist. For example, PhCs exhibit some angular discrimination of light, but this discrimination is always strongly dependent on frequency, as illustrated in Fig. 1b. In this letter, we present a material-system that opens precisely the desired angular gaps, as shown in Fig. 1c. For example, using realistic constituent material parameters, we present numerical calculations demonstrating an angular photonic bandgap (PBG) material-system in which light close to normal incidence is nearly perfectly transmitted for a wide range of frequencies, independent of the polarization. In contrast, light of angles further from the normal

(e.g. $[22.5^{\circ}-90^{\circ}]$) can be nearly perfectly reflected over $> 100\%$ fractional frequency bandgap. The key to these novel angular PBG material-systems is exploring PhCs whose constituents have anisotropic permittivity and/or permeability.

To demonstrate the fundamental physics principle at work here, we first show in Fig. 2a an angular PBG material-system that opens an angular gap for the TM (electric field is in the plane of incidence) polarization and certain frequency range only. In this example, we take layer A to have an anisotropic effective permittivity $\epsilon_A = (1.23, 1.23, 2.43)$ whereas layer B has isotropic permittivity $\epsilon_B = 1.23$. To accomplish the required anisotropy, one could either use naturally anisotropic materials³ such as TiO_2 , or explore metamaterial approaches. An example of a metamaterial system that in the long wavelength limit possesses an effective epsilon of $(1.23, 1.23, 2.43)$ is shown to the left of the inset of Fig. 2a, and consists of a two dimensional (2D) periodic square lattice of dielectric rods having radius $r = 0.2d$ where d (the in-plane period) equals $d = 0.1a$ (a is the thickness of each bilayer⁴), and made out of an isotropic material with⁵ $\epsilon_{\text{rods}} = 12.25$. To the right of the inset of Fig. 2a, we show a schematic diagram of normally incident TM-(in blue) and TE-(in red) polarized light incident on the above-described multilayer. Since \vec{E} lies in the xy -plane, both polarizations experience $n_A = n_B = \sqrt{1.23}$, so because of the absence of any contrast in the refractive index, there is no photonic bandgap and normally incident light of all frequencies and both polarizations gets transmitted, apart for the small reflections at boundaries between the structure and air. As seen in Fig. 2b, the situation changes with oblique incidence: TM-polarized light now has $E_z \neq 0$, and thus experiences an index contrast ($n_A^{\text{TM}} \neq n_B^{\text{TM}} = \sqrt{1.23}$); therefore, a photonic bandgap opens, with strong reflections for TM light. In contrast, a TE-polarized light incident at oblique angle still has $E_z = 0$ and thus experiences no index contrast as shown (Fig. 2b: $n_A = n_B = \sqrt{1.23}$); therefore, it gets transmitted for all frequencies. Thereby, TM light is transmitted for small θ_{inc} and reflected for large θ_{inc} . This structure works only for a certain frequency range (9.3% in the case of Fig. 2b). Later in the letter, we show how to generalize our approach to both polarizations and wide frequency ranges.

It is useful to look at analytical expressions for the effective refractive index n_A of the anisotropic layer. A simple calculation starting from Maxwell's equations⁶ yields the following refractive indices ($n = c/v_{\text{phase}}$) experienced by TE and TM light respectively in the anisotropic layer A:

$$n_A^{TE} = \frac{1}{\sqrt{\frac{\cos^2 \theta_A^{TE}}{\mu_{xx}^A \epsilon_{yy}^A / \mu_0 \epsilon_0} + \frac{\sin^2 \theta_A^{TE}}{\mu_{zz}^A \epsilon_{yy}^A / \mu_0 \epsilon_0}}} \quad (1)$$

$$n_A^{TM} = \frac{1}{\sqrt{\frac{\cos^2 \theta_A^{TM}}{\mu_{yy}^A \epsilon_{xx}^A / \mu_0 \epsilon_0} + \frac{\sin^2 \theta_A^{TM}}{\mu_{yy}^A \epsilon_{zz}^A / \mu_0 \epsilon_0}}} \quad (2)$$

where θ_A^{TE} and θ_A^{TM} are refraction angles for TE and TM polarizations in layer A, as described by Snell's law:

$$n_A^{TE} \sin \theta_A^{TE} = n_{air} \sin \theta_{inc} \quad (3)$$

$$n_A^{TM} \sin \theta_A^{TM} = n_{air} \sin \theta_{inc} \quad (4)$$

From Eqs. (1) and (2), we see that TE light is affected only by ϵ_A^{yy} , μ_A^{xx} , and μ_A^{zz} , while TM light is affected only by μ_A^{yy} , ϵ_A^{xx} and ϵ_A^{zz} . In particular, TM light is affected by ϵ_A^{zz} , in contrast to the TE polarization. We also note that for near-normal incidence, $\sin \theta_A \approx 0$, so n_A increases only slightly with increasing anisotropy. However, for incidence angles not close to the normal, n_A increases more rapidly with increasing anisotropy, and therefore higher anisotropy in ϵ or μ results in higher index contrast and wider frequency gaps at those angles.

To achieve a simultaneous bandgap for both TE and TM polarizations, we consider a multilayer structure with anisotropy in both permittivity and permeability tensors: $\epsilon_B = \mu_A = \gamma_1$ while $\epsilon_A = \mu_B = (\gamma_1, \gamma_1, \gamma_2)^T$. For simplicity, we consider the case $\epsilon_{inc} = \mu_{inc} = \gamma_1$ here. TM light with oblique incidence from air experiences a photonic bandgap, because $n_B^{TM} = \sqrt{\gamma_1}$ while $n_A^{TM} \neq \sqrt{\gamma_1}$ (Eq. 2). On the other hand, TE incidence at the same angle also experiences an index contrast because $n_A^{TE} = \sqrt{\gamma_1}$ while $n_B^{TE} \neq \sqrt{\gamma_1}$ (Eq. 1). The relative size of the TE (and also TM) gap as a function of θ_{inc} and the degree of anisotropy γ_2/γ_1 was obtained from the TMM⁸, and shown in Fig. 3; the thickness of layers A and B were chosen to be equal ($h_A = h_B = 0.5a$) so that the structure discriminates angles equally, over the same frequency interval and for both polarizations simultaneously⁹. From the contour plot, we observe that the size of the fractional gap increases only slightly with increasing anisotropy γ_2/γ_1 beyond $\gamma_2/\gamma_1 \approx 2$, which can also be seen by inspection of Eq. (1) and Eq. (2), and noticing that the achievable index contrast

“saturates” for large γ_2/γ_1 anisotropy values. Therefore, materials with very large anisotropy do not necessarily lead to much larger bandgaps in these structures. This is somewhat contrary to conventional PhCs where large index contrasts typically lead to larger bandgaps. Note also that the size of the fractional frequency gap increases with θ_{inc} .

Having proposed a structure that opens an angular gap for both polarizations over a certain frequency range, we now discuss a path as to how one might enlarge the frequency range over which this angular discrimination is exhibited. Since we are concerned with the largest fractional frequency gap that occurs simultaneously for both polarizations, we operate at quarter-wave condition. We use anisotropic $\epsilon_A = \mu_A$ (as opposed to the previously considered case when we had anisotropic $\epsilon_A = \mu_B$). We start with a single stack consisting of 130 homogeneous bilayers with $\epsilon_A = \mu_A = (1.23, 1.23, 2.43)$ and $\epsilon_B = \mu_B = 1.23$. The size of each bilayer in this stack is a . Light incident at 22.5° (from air) on this stack experiences a simultaneous TE and TM photonic bandgap having a fractional frequency width of 1.64% (at quarter-wave condition). To widen this fractional frequency range, we consider a multilayer consisting of 71 such stacks, each stack being made out of 130 bilayers. However, the period of each stack is graded, so that frequency gaps of different stacks are contiguous and merge together, resulting in a much larger frequency gap (≈ 71 times the size of the gap in the single gap case). More specifically, we choose the period a_i of the i^{th} stack ($i = 1, 2, \dots, 71$) to be $a_i = 1.0164^{(i-1)}a$, where a is the period of the first stack facing the incident light. We also choose the thickness h_A^i of layer A in the i^{th} stack to be $0.494a_i$ so that the quarter-wave condition (which maximizes the relative size of the frequency gap) is satisfied. In Fig. 4a, TMM results for the transmission spectrum at 22.5° incidence on the 71-stack multilayer show a reflection window of relative frequency size of $\approx 107\%$ for both TE and TM polarizations. In Fig. 4b, we show TMM results for light incident at 45° on this same structure: nearly complete reflection occurs inside the reflection window for 22.5° incidence (Fig. 4a), indicating a large angular bandgap. In fact, this proposed structure exhibits an angular gap (for θ_{inc} between 22.5° and 90°) for both polarizations simultaneously over a 107% wide frequency range (Fig. 1c).

Applicability of the angular PBG concept we propose for a given application of interest will depend on the availability of anisotropic materials in the frequency range of interest. Besides the dielectric metamaterial for TM polarized light (c.f. Fig. 2a), amorphous photonic crystals could be of interest^{10,11}. To achieve polarization independence (where anisotropic μ is needed),

one can exploit metallo-dielectric metamaterials¹². Another option is to split incoming light according to polarization before it enters the structure, rotate TE polarization into TM polarization, and only then allow it to continue onto our structure¹³.

In summary, we presented a novel class of material-systems, capable of discriminating light primarily based on the angle of incidence. Angular PBG material-systems of this type could potentially find uses in applications where radiation is incoming from a known, defined direction, and it is desirable to prevent subsequent “escape” of radiation energy. As an avenue of further research, it would be interesting to explore whether material-systems of similar properties could one day be useful for solar energy applications. Sun light has a well defined angle of incidence. A portion of sun light is reflected from solar-energy conversion devices, while a portion is re-radiated (either because of radiative recombination, or in solar-thermal¹⁴ systems because of thermal emission); this represents losses, which can often be substantial. If one could place a material-system that would allow light at one particular angle (the one coming from the sun) to get perfectly through, while light emerging from the device (most of which typically propagates at different angles) would be reflected back to the device, the efficiency of the solar-energy conversion could be improved^{15,16,17,18}.

We would like to acknowledge helpful discussions with Dr. Zheng Wang, Prof. John D. Joannopoulos, Dr. Peter Bermel and Prof. Jorge Bravo-Abad. This work was supported in part by the MRSEC program of National Science Foundation under Award No. DMR-0819762. R. H. was supported as part of the S3TEC, an Energy Frontier Research Center funded by the U.S. Department of Energy, Office of Science, Office of Basic Energy Sciences under Award Number DE-SC0001299. The authors thank the MIT Energy Initiative for their financial support.

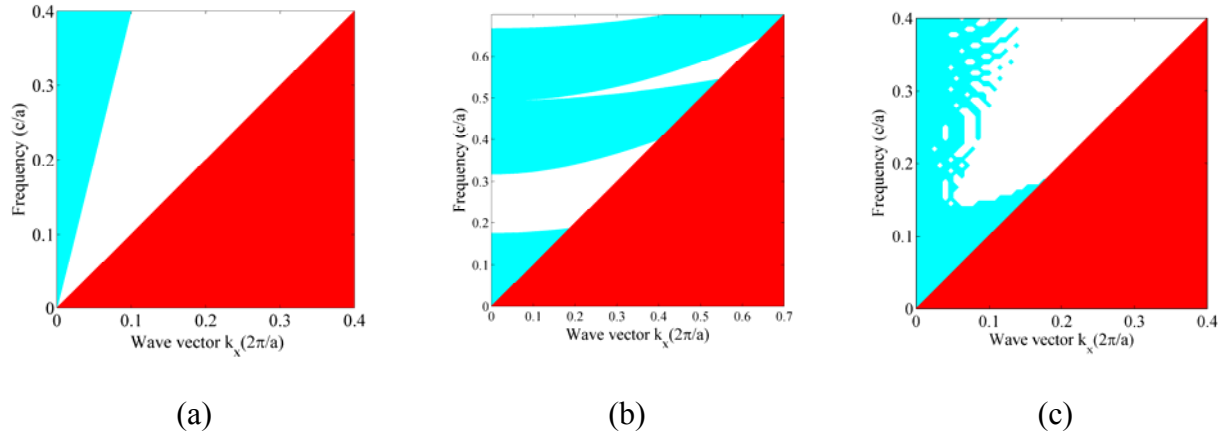


FIG 1: (Color online) Dispersion diagrams for three different angularly selective systems. k_x denotes transverse incident wave vector; modes below the light line (red) are evanescent in the incident medium (air), and hence are not of interest here. White denotes modes of the given ω and k_x which are strongly reflected. (a) An ideal “angular photonic bandgap” system: light of incoming angle $|\theta_{\text{inc}}| > \text{asin}(0.1/0.4) \approx 14.5^\circ$ is strongly reflected, irrespective of ω . Ideally, modes denoted with blue would be nearly perfectly transmitted. (b) s-polarized light incident on a 1D photonic crystal (a quarter-wave stack of materials with $\epsilon=13$ and $\epsilon=2$). Angular discrimination is associated with strong frequency-dependence. (c) Angular selectivity of a material-system presented in this letter (details in Figure 4), with an ideal angular photonic bandgap; “a” is the period of the top-most periodic stack of our structure (as discussed in Figure 4).

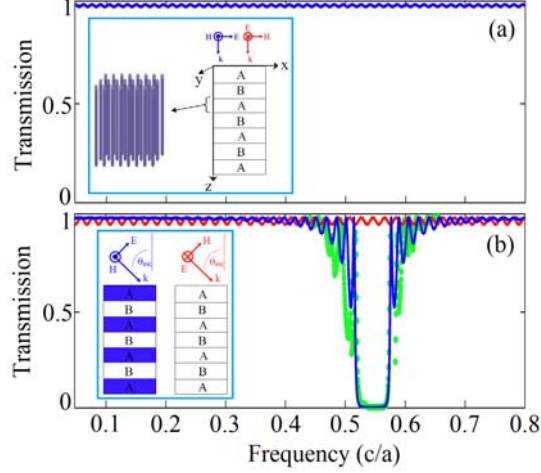


FIG. 2: (Color online) (a) Transmission spectra (obtained from the transfer matrix method (TMM)¹¹) for TE-(red) and TM-(blue) polarized light normally incident from air on 30 bilayers of the structure shown in the inset. (b) Schematic diagrams showing TM-(inset, left) and TE-(inset, right) polarized light incident at nonzero angle from air ($n_{\text{inc}}=1$). The physical structure considered in this figure is always the same; however, TM light incident at nonzero angle “sees” a structure of different optical properties than the structure “seen” by either TM light incident normally, or by TE light incident at any angle. Transmission spectra (obtained from TMM) for TE-(red) and TM-(blue) polarized light incident at 45° from air on 30 bilayers of the structure shown in the inset. Green curve: Transmission spectrum (obtained from the FDTD¹⁹ method) for TM-polarized light incident at 45° from air on 30 bilayers of the structure in the inset, in the case when anisotropic layer A is not made from a homogeneous material, but is a metamaterial implemented from a square lattice of dielectric rods. A TM photonic bandgap opens and closely overlaps with the TM gap obtained from TMM for the uniform dielectric case; as expected, TMM is a good approximation for analyzing the structures of this type.

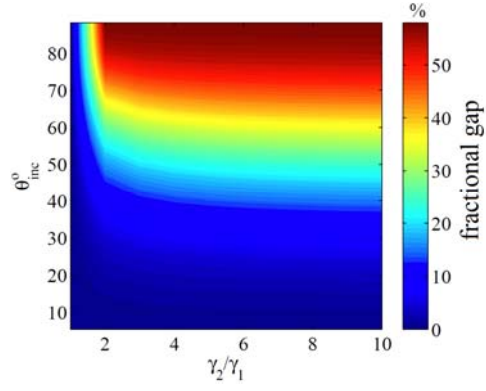


FIG. 3: (Color online) The relative size of the TE gap as a function of θ_{inc}^0 and γ_2/γ_1 for a multilayer structure that has $\epsilon_A = \mu_B = (\gamma_1, \gamma_1, \gamma_2)$, $\epsilon_B = \mu_A = \gamma_1$. The light is incident from a medium of $\epsilon_{\text{inc}} = \mu_{\text{inc}} = \gamma_1$. The TM gap is identical to the TE gap.

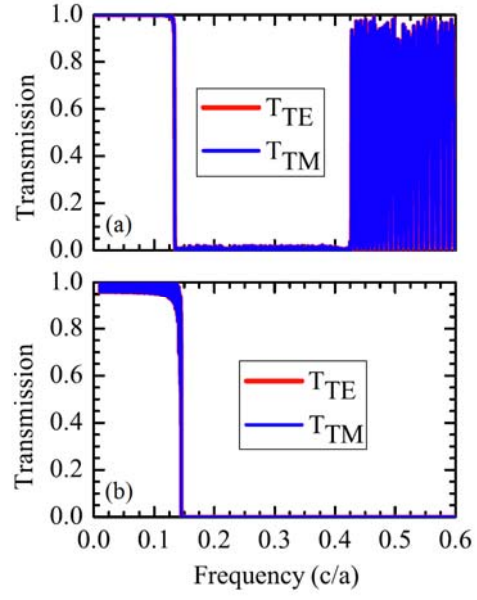


FIG. 4: (Color online) Transmission spectra of the graded-periodicity multilayer stack at various incident angles: (a) 22.5° and (b) 45° .

REFERENCES

-
- ¹ Eugene Hecht, *Optics*, Chapter 8 (pages 331-339), Fourth Edition, (Addison-Wesley, 2002)
- ² John D. Joannopoulos, Steven G. Johnson, Joshua N. Winn, and Robert D. Meade, *Photonic Crystals: Molding the Flow of Light*, second edition (Princeton University Press, 2008).
- ³ Pochi Yeh, *Optical Waves in Layered Media*, Chapter 9 page 209 (John Wiley & Sons Inc, 1988).
- ⁴ Since we know that a TM reflection window opens at 45° , we choose the relative thickness h_A of layer A such as to maximize the size of the TM fractional gap, which happens at the quarter-wave condition ($h_A n_A \cos(\theta_A^{\text{TM}}) \omega_0/c = h_B n_B \cos(\theta_B^{\text{TM}}) \omega_0/c$), ω_0 being the central frequency of the gap. This results in $h_A = 0.46a$.
- ⁵ In a 2D square lattice of dielectric rods, modes having their E-field along the rods are substantially more concentrated inside the rods and therefore experience the high E of the rods. On the other hand, modes having their E-field in the periodicity plane experience average E smaller than that along the rods, hence the anisotropy in effective ϵ . Our frequency domain simulations (not discussed here) show that in the low frequency limit, the metamaterial indeed has effective $\epsilon = (1.23, 1.23, 2.43)$.
- ⁶ Pochi Yeh, *Optical Waves in Layered Media*, Chapter 9 pages 201-213 (John Wiley & Sons Inc, 1988).
- ⁷ Note that a structure having $\epsilon_A = \mu_A = (\gamma_1, \gamma_1, \gamma_2)$ and $\epsilon_B = \mu_B = \gamma_1$ would work equally well. However, the structure that we analyze in Fig. 3 offers somewhat more flexibility in the material choice, in the sense that equal anisotropic ϵ and μ do not have to occur in the same material.
- ⁸ Pochi Yeh, *Optical Waves in Layered Media*, Chapter 5 (pages 102-110) and Chapter 6 (pages 118-128) (John Wiley & Sons Inc, 1988). In TMM, we model each layer as being uniform; e.g. in the case of layer A of Fig. 2, uniform $\epsilon = (1.23, 1.23, 2.43)$.
- ⁹ Note that this choice of $h_A = h_B$ does not result in the largest possible fractional gap for either polarization, which actually occurs at the quarter-wave condition, satisfied non-simultaneously for the two different polarizations when $\epsilon_A = \mu_B = (\gamma_1, \gamma_1, \gamma_2 = \gamma_1)$.
- ¹⁰ M. Rechtsman, A. Szameit, F. Dreisow, M. Heinrich, R. Keil, S. Nolte, and M. Segev, "Band Gaps in Amorphous Photonic Lattices," in *Quantum Electronics and Laser Science Conference*, OSA Technical Digest (CD) (Optical Society of America, 2010), paper QMG1.
- ¹¹ Jin-Kyu Yang, Carl F. Schreck, Heeso Noh, Seng-Fatt Liew, Mikhael I. Guy, Corey S. O'Hern, Hui Cao, arXiv:1008.4804v1 [cond-mat.dis-nn].
- ¹² J. B. Pendry, A. J. Holden, D. J. Roddins, and W. J. Stewart, *IEEE transactions on microwave theory and techniques* **47**, NO. 11, November 1999.
- ¹³ T. Barwicz, M. R. Watts, M. A. Popovic, P. T. Rakich, L. Socci, F. X. Kaertner, E. P. Ippen, and H. I. Smith, *Nature Photonics*, **1**, 57, (2007).

-
- ¹⁴ E. Rephaeli, and S. Fan, *Appl. Phys. Lett.* **92**, 211107, (2008).
- ¹⁵ Marian Florescu, Hwang Lee, Irina Puscasu, Martin Pralle, Lucia Florescu, David Z. Ting and Jonathan P. Dowling, *Solar Energy Materials and Solar Cells* **91**, 1599-1610 (2007).
- ¹⁶ Martin A. Green, *Progress in photovoltaics* **9**, 257-261 (2001).
- ¹⁷ Stephan Fahr, Carolin Ulbrich, Thomas Kirchartz, Uwe Rau, Carsten Rockstuhl, and Falk Lederer, *Optics Express* **16**, 9332-9343 (2008).
- ¹⁸ C. Ulbrich, S. Fahr, M. Peters, J. Upping, T. Kirchartz, C. Rockstuhl, J. C. Goldschmidt, P. Loper, R. Wehrspohn, A. Gombert, F. Lederer, and U. Rau, *Photonics for Solar Energy Systems II* **7002**, 70020A (2008).
- ¹⁹ Ardavan Farjadpour, David Roundy, Alejandro Rodriguez, Mihai Ibanescu, Peter Bermel, J. D. Joannopoulos, Steven G. Johnson, and Geoffrey Burr, *Opt. Lett.* **31**, 2972-2974 (2006).